

Rotation of Transition Metal Ions under Electric Fields: Possible New Superconducting Electron Pairing Mechanism

Tiege Zhou*

(College of Electronic Information and Optical Engineering, Nankai University, 300350 Tianjin, P. R. China)

Abstract

Electric field effects in iron- and copper-based superconductors were studied by using the first-principles calculations based on the density functional theory (DFT). The research objects include iron-based superconductors (KFe_2Se_2 , LaFeAsO , NdFeAsO , and BaFe_2As_2) and copper-based superconductors ($\text{YBa}_2\text{Cu}_3\text{O}_7$, $\text{HgBa}_2\text{Ca}_2\text{Cu}_3\text{O}_8$, $\text{Tl}_2\text{Ba}_2\text{CaCu}_2\text{O}_8$, and $\text{Bi}_2\text{Sr}_2\text{Ca}_2\text{Cu}_3\text{O}_{10}$). To describe the strong correlation effect of $3d$ -electrons or $4f$ -electrons, the GGA+U method was used. Some results were further verified by the HSE method. The densities of states (DOS) were given. The change of the charge densities under electric fields is presented to demonstrate the electric field effect. It is found that the electron clouds of Fe ions in iron-based superconductors, Nd ions in $\text{Nd}_2\text{Fe}_2\text{As}_2\text{O}_2$, and Cu ions in copper-based superconductors change obviously. The pattern of the change is more like a rigid-body rotation than an elastic deformation. The author proposed that the rotation of the electron clouds of transition metal ions may be a new medium of superconducting electron pairing. The author's views about some issues and suggestions on follow-up studies are also presented.

Keywords: high temperature superconductivity; electric field effect; electron pairing mechanism; electron cloud rotation

1. Introduction

In 1986, J. G. Bednorz and K. A. Müller discovered that there may be high-temperature superconductivity (HTS) in La-Ba-Cu-O oxides^[1], which revealed a new chapter in the research of superconductivity. In 1987, M. K. Wu et al.^[2] and Z. X. Zhao et al.^[3] synthesized Y-Ba-Cu-O superconductors, respectively, almost at the same time. The critical temperature (T_c) for superconductivity reached 90K and achieved a breakthrough above the liquid nitrogen temperature. In 1988, H. Maeda, Y. Tanaka, M. Fukutumi, and T. Asano. found BiSrCaCuO superconductors with a T_c above 100K^[4]. In 1988, Z. Z. Sheng et al. synthesized Tl-containing superconductors^{[5][6]}. In 1993, $\text{HgBa}_2\text{CuO}_{4+\delta}$, the first member of the Hg series, was synthesized by S. N. Putilin et al., with a T_c of 94K^[7]. In 1993, A. Schilling et al. synthesized

* E-mail: zhoutg@nankai.edu.cn

HgBa₂Ca₂Cu₃O_{8+δ}, raising the T_c above 130K^[8]. The T_c of Hg-1223 can reach 153 K under a high pressure^[9]. In addition to copper-based superconductors, iron-based superconductors have also received widespread attention^{[10][11][12]}. The T_c of PrFeAsO_{0.89}F_{0.11} reaches 52K^[13] and SmFeAsO_{0.85} 55K^[14]. In 2012, Q. K. Xue et al. successfully grow FeSe thin films with one unit-cell thickness on the surface of SrTiO₃ substrates by the MBE method^[15]. The monolayer FeSe showed a T_c above the liquid nitrogen temperature (77K). In 2014, Q. K. Xue et al. reported the FeSe monolayer with a T_c over 100K^[16].

The discovery of copper- and iron-based superconductors has seriously challenged the BCS theory, because BCS theory predicts that T_c cannot be so high. Traditional electron-phonon interaction mechanism failed to explain the electron pairing mechanism and other new phenomena exhibited in copper- and iron-based superconductors. In 1987, P. W. Anderson^[17] has put forward the famous RVB model for copper-based superconductors. Though many theories^{[18][19][20]} have been proposed so far, the electron pairing mechanism is still under intense debate. Anderson^[21] made it clear in 2007 that many theories about high-temperature superconducting electron pairing mechanism might be in the wrong direction.

The author believes, to explain the electron pairing mechanism in high-temperature superconductors, we must go back to the traditional electron pairing mechanism. As early as 1950, H. Fröhlich^[22] proposed that electron-lattice interaction is the source of superconductivity, supported by the isotope effect^{[23][24]}. Based on this, the well-known BCS theory^{[25][26]} was developed, explaining the traditional superconductivity successfully. The author argues that the electronic-phonon interaction in BCS theory is closer to a mathematical tool than a simple and intuitive physical model. The simple and intuitive model is as follows. The electric field of an electron will distort the ions' positions. When the electron leaves, the ions will not restore to the original positions immediately. This results in a positive charge region which will attract another electron and thus creates an attractive interaction between electrons. Based on the above consideration, the author believes that a study of the influence of electric fields on copper- and iron-based superconductors may provide important information about the electron pairing mechanism. Although many experiments of HTS under electric fields have been conducted^{[27][28][29]}, the main purpose is to change the carrier concentration and thus the superconducting properties. It is related to new superconducting device preparation, no electron pairing mechanism involved. In the study of the electric field effect of eight typical unconventional superconductors, the author found, for the first time, the electron cloud of transition metal ions behaves like a rigid-body rotation. Based on this discovery, the author proposes a possible new superconducting electron pairing mechanism. This article describes the research methods, results, possible new superconducting electron pairing mechanism, and the authors' views on several issues about HTS.

2. Research objects and calculation methods

The author selected four typical iron-based superconductors (KFe_2Se_2 , LaFeAsO , NdFeAsO and BaFe_2As_2) and four typical copper-based superconductors ($\text{YBa}_2\text{Cu}_3\text{O}_7$, $\text{HgBa}_2\text{Ca}_2\text{Cu}_3\text{O}_8$, $\text{Tl}_2\text{Ba}_2\text{CaCu}_2\text{O}_8$ and $\text{Bi}_2\text{Sr}_2\text{Ca}_2\text{Cu}_3\text{O}_{10}$). It is worth noting that the objects calculated are not strictly actual superconductors. They are parent materials, and the author makes them closer to the actual superconductors by changing the stoichiometries or valence electron numbers.

The first-principles calculation based on DFT was used. Most of the calculations were conducted within the Vienna Ab-initio Simulation Package (VASP) ^[30] ^[31]. The projector augmented plane wave (PAW) method ^[32]^[33] was used to describe the interaction between the valence electrons and the ion cores. The generalized gradient approximation (GGA) of Perdew-Burke-Ernzerhof (PBE) ^[34] was used for the exchange correlation potential. To describe the strong correlation of the $3d$ or $4f$ electrons, the GGA+U method is used. For the $3d$ orbitals of Fe and Cu, the U_{eff} values are 4eV ^[35] and 6.5eV ^[36]^[37], respectively. Plane waves were used to expand the valence electron wave functions. The cutoff energy is set to 400 eV which has been tested by taking both accuracy and computing cost into account. The valence electron configurations of the pseudopotentials are taken as $3p^63d^74s^1$ for Fe (with a radius of 2.200 a.u.), $4s^24p^4$ for Se, $3s^23p^64s^1$ for K, $5s^25p^65d^16s^2$ for La, $4s^24p^3$ for As, $4f^45s^25p^66s^2$ for Nd, $5s^25p^66s^2$ for Ba, $5d^{10}6s^2$ for Hg, $3s^23p^64s^2$ for Ca, $3p^63d^{10}4s^1$ for Cu (with a radius of 2.000 a.u.), $2s^22p^4$ for O, $4s^24p^64d^15s^2$ for Y, $5d^{10}6s^26p^1$ for Tl, $5d^{10}6s^26p^3$ for Bi, and $4s^24p^65s^2$ for Sr. For some results, further calculations with the Heyd, Scuseria, and Ernzerhof (HSE) ^[38] hybrid-functional were performed for cross validation.

Quantum Espresso (QE) simulation package^[39] and norm-conserving pseudopotentials were employed in the calculation of iron-based superconductors under uniform electric fields. The valence electron configurations of the pseudopotentials are taken as $3s^23p^63d^64s^2$ for Fe (with a radius of 1.909 a.u.), $4s^24p^4$ for Se, $3s^23p^64s^1$ for K, $5s^25p^65d^16s^2$ for La, $4s^24p^3$ for As, $3s^23p^64s^1$ for Ba, and $2s^22p^4$ for O. Pseudopotentials with less valence electrons ($3d^64s^2$ for Fe, $4s^1$ for K, and $6s^2$ for Ba) were also used for comparison. The cut-off energy of the plane wave is set to 80 Ry . The exchange-correlation interaction of electrons is described by the GGA+U method. U_{eff} is 6.5 eV for the $3d$ orbital of Fe. Set occupations = 'fixed' in the input file. In general, occupations = 'fixed' cannot be used for metal. Considering that the calculated objects are not good conductors, it is acceptable in the calculation of uniform electric fields, but it is difficult to converge to a high accuracy. In the following, the author will give an explanation.

The results given below without description are obtained with VASP. When the QE software package is used, the author will point out. First, the geometry of the system is optimized until all forces on ions are less than 0.01 eV/\AA . After optimization, the influence of an electric field on the

charge density is calculated. Calculations of iron- and copper-based superconductors were converged to 10^{-5} eV and 10^{-6} , respectively, for the tolerance on the total energy. There are three ways of applying an electric field to the system. The first is to insert one Li^+ ion at an appropriate position (denoted by Li^+ Insertion); the second is to slightly change the position of some atom (Slight Change); and the third is to apply a uniform electric field (Uniform E-field) with QE package.

3. Results and discussion

3.1 $\text{K}_2\text{Fe}_4\text{Se}_4\text{-2e}$ and $\text{K}_2\text{Fe}_4\text{Se}_4$

KFeSe superconductors have different stoichiometries, such as $\text{K}_{0.8}\text{Fe}_{1.6}\text{Se}_2$ ^[40] and $\text{K}_x\text{Fe}_2\text{Se}_2$ ^[41]. The T_c of $\text{K}_{0.8}\text{Fe}_{1.6}\text{Se}_2$ is 31.8K. To access an antiferromagnetic state, the author adopts $\text{K}_2\text{Fe}_4\text{Se}_4$ for calculation. Two cases were calculated. One is $\text{K}_2\text{Fe}_4\text{Se}_4\text{-2e}$, with two valence electrons subtracted, in which the valence of K is +1, Se is -2, and Fe is +2. The other is $\text{K}_2\text{Fe}_4\text{Se}_4$, no electron added or subtracted, in which the valence states are rather complicated. If K is +1 and Se is -2, then Fe is +3/2. The k -point is set to $10 \times 10 \times 4$ when using the GGA+U method, and $6 \times 6 \times 2$ when using the HSE method. Fig. 1 shows the DOS of $\text{K}_2\text{Fe}_4\text{Se}_4\text{-2e}$, in which the 3d orbital of the Fe ion (Fe_d) is also presented. It's an insulator, and the GGA+U method is in very good agreement with the HSE method except the bandgap. The GGA+U method gives a bandgap of about 1.3 eV, whereas the HSE method gives a bandgap of about 1.8 eV.

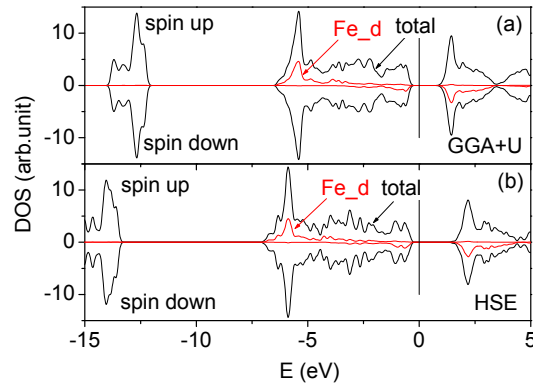


Fig. 1 DOS of $\text{K}_2\text{Fe}_4\text{Se}_4\text{-2e}$ from GGA+U (a) and HSE (b) method

All the three methods were employed to study the influence of electric fields. The fractional coordinate of the inserted Li^+ ion is (0.5, 0.5, 0.62) and it is 2.55 Å away from the nearest neighbor Fe, 2.73 Å from Se, and 1.5 Å from K. The original position the Se atom to be changed is (0.5, 0.5, 0.8682) and then revised to (0.5, 0.5, 0.8602). The position was changed in the (001) direction by -0.1 Å. When applying the uniform electric field, QE package is used and the k -point is set to $6 \times 6 \times 2$. The uniform electric field is along (111) direction, with a value of 0.00087 Ry a.u.. Set $\text{efield_cart}(1) = 0.0005$ Ry a.u., $\text{efield_cart}(2) = 0.0005$, and $\text{efield_cart}(3) = 0.0005$ in the

main input file. The convergence accuracy reaches 3×10^{-4} Ha. When the k -point is reduced to $3 \times 3 \times 1$, the convergence can reach 1×10^{-5} Ha, and the result is in accordance with that of $6 \times 6 \times 2$ k -point.

Fig. 2 displays the crystal structure, spin density map and the charge density difference (CDD) with and without electric fields. The yellow color represents a positive value or increase of the charge density, while the blue color negative or decrease. It can be seen from the spin density map that there is a clear spin distribution on the iron ions and the antiferromagnetic state is present. For the three ways of exerting influence of electric field, the charge density around Fe ions changes significantly. There is no similar change around other atoms. The change is more like a rigid rotation rather than an elastic deformation, because the change is not entirely along the direction of the electric field. Some areas increase, while some areas decrease. Furthermore, the pattern of the change is like $3d$ electron clouds. The isosurface of the CDD is equal to that of the spin density, indicating the rotation is obvious. The author is sure that the observed results were not caused by low computational accuracy, from calculations with different accuracies.

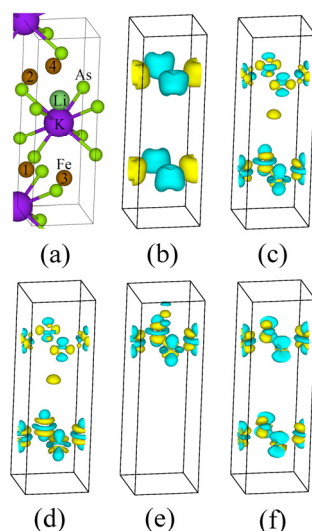


Fig. 2 (a) Crystal structure of $K_2Fe_4Se_4$ with one Li^+ ion inserted; (b) Spin density map (GGA+U, iso = 0.02 num_electron/bohr³); (c) CDD from Li^+ Insertion (GGA+U, iso = 0.02); (d) CDD from Li^+ Insertion (HSE, iso = 0.02); (e) CDD from Slight Change (GGA+U, iso = 0.02); (f) CDD from Uniform E-field (QE, GGA+U, iso = 0.02). iso represents isosurface.

Table 1 shows the local magnetic moments (LMM) of the Fe ions in $K_2Fe_4Se_4-2e$. When there is no electric field, LMM from the GGA+U method is very close to that from the HSE method, showing the consistency of the two methods. For the results from QE package, LMMs from the low accuracy and high k -point calculation are consistent with those from the high accuracy and low k -point calculation, indicating a converge of 3×10^{-4} Ha is reasonable. The change of LMMs with and without electric fields is small, which indicates the electric field did not change the nature of the system significantly.

Table 1 LMM (μB) of Fe atoms in $\text{K}_2\text{Fe}_4\text{Se}_4\text{-2e}$

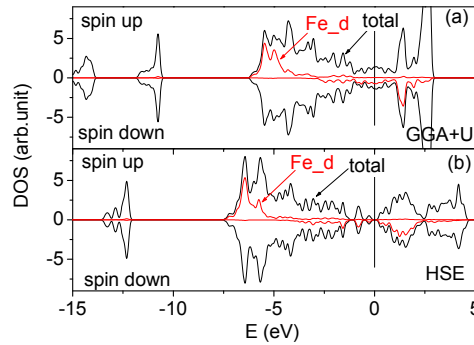
| | Method | Fe1 | Fe2 | Fe3 | Fe4 |
|-----------------|-------------------------|-------|-------|--------|--------|
| GGA+U | No field | 3.384 | 3.384 | -3.384 | -3.384 |
| | Li^+ Insertion | 3.453 | 3.322 | -3.599 | -3.274 |
| | Slight Change | 3.388 | 3.361 | -3.385 | -3.441 |
| HSE | No field | 3.376 | 3.376 | -3.376 | -3.376 |
| | Li^+ Insertion | 3.481 | 3.273 | -3.507 | -3.237 |
| QE(662k) | No field | 3.229 | 3.229 | -3.193 | -3.193 |
| | Uniform E-field | 3.276 | 3.301 | -3.295 | -3.299 |
| QE(331k) | No field | 3.227 | 3.227 | -3.227 | -3.227 |
| | Uniform E-field | 3.289 | 3.289 | -3.289 | -3.289 |

In addition, increasing or decreasing the lattice constant by 2.5%, the same rotation can be observed. For Figure 2 (c), increasing the plane wave cutoff energy to 500eV, the results are consistent with that of 400eV. Calculations with valence electrons as $3d^6 4s^2$ (1.9915 a.u.) for Fe and $4s^1$ for K were performed. The k -point is $6 \times 6 \times 2$ and the convergence reaches 1×10^{-6} Ha. The results are consistent with the previous, showing the observed rotation comes from the $3d$ electrons mainly.

For $\text{K}_2\text{Fe}_4\text{Se}_4$, with no electron subtracted or added, the results show that there is also a significant rotation of the electron cloud of the Fe ions.

3.2 LaFeAsO

The author calculated $(\text{LaFeAsO})_2$ directly, without increase or decrease of the number of the valence electrons. For the GGA+U method, the k -point is set to $10 \times 10 \times 6$. For the HSE method, the k -point is set to $6 \times 6 \times 2$. Fig. 3 shows the DOS. The two methods give similar DOS for the d -orbitals of the Fe atoms.

Fig. 3 DOS of $(\text{LaFeAsO})_2$ from GGA+U (a) and HSE (b) method

When calculating the influence of electric field, the coordinate of the inserted Li^+ ion is (0.58,

0.58, 0.62). The Li^+ ion is 1.877Å, 1.979Å, and 2.407Å from the nearest neighbor Fe atom, As atom, and La atom, respectively. The original coordinate of the As atom to be changed is (0.75, 0.75, 0.3363), and then revised to (0.75, 0.75, 0.3113). The position was changed in the (001) direction by -0.22 Å. When using the QE package, the k -point is set to $6 \times 6 \times 2$. The convergence reaches 1×10^{-5} Ha. Fig. 4 shows the crystal structure, CDDs and the total charge density ($3d^6 4s^2$ are taken as valence electrons for Fe).

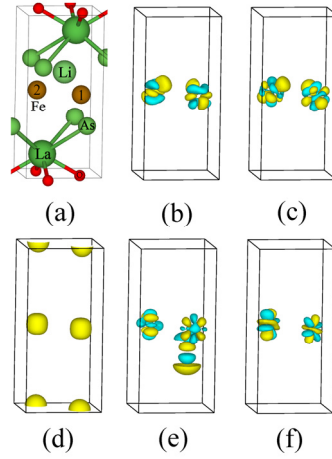


Fig. 4 (a) Crystal structure of $(\text{LaFeAsO})_2$ with one Li^+ ion inserted; (b) CDD from Li^+ Insertion (GGA+U, iso = 0.02) ; (c) CDD from Li^+ insertion (HSE, iso = 0.02); (d) Total charge density (GGA+U, iso = 0.3); (e) CDD from Slight Change (HSE, iso = 0.02); (f) CDD from Uniform E-field (QE, iso = 0.02)

It can be seen from all the CDDs that there is a significant rotation of the electron clouds of the Fe ions. From Fig. 4(d), the distribution of the charge density around the iron atom does not have a perfect spherical symmetry. The author believes that this is the main reason for the rotation under electric fields.

LMMs are given in Table 2. The results given by different methods are consistent, and the applied electric field has little effect on the local magnetic moments.

Table 2 LMM of Fe in $(\text{LaFeAsO})_2$

| Method | | Fe1 | Fe2 |
|--------------|-------------------------|-------|--------|
| GGA+U | No field | 3.261 | -3.261 |
| | Li^+ Insertion | 3.286 | -3.287 |
| | Slight Change | 3.280 | -3.332 |
| HSE | No field | 3.282 | -3.282 |
| | Li^+ Insertion | 3.244 | -3.244 |
| | Slight Change | 3.349 | -3.360 |
| QE | No field | 3.232 | -3.222 |
| | Uniform E-field | 3.219 | -3.230 |

The calculation with $3d^64s^2$ as valence electrons for Fe shows that there is a significant rotation of the electron cloud. Increasing the cut off energy of the plane wave to 500 eV gives the same results as 400 eV. The author also observed obvious rotation when 0.2 electrons added.

In addition, the author calculated a $6 \times 2 \times 1$ supercell. The position of the inserted Li^+ ion is (0.79, 0.38, 0.58); the coordinate of the As atom to be changed was (0.2083, 0.6250, 0.6637) and decreased by 0.01 (0.082 Å) in the y direction. Fig. 5 shows the CDDs. The most important discovery is significant rotation occurs far away from the position where the electric field is applied. This shows that electron clouds of Fe ions in iron-based superconductors are more sensitive to the electric field, which is different from that of copper-based superconductors given below. The electron clouds of some Fe ions change obviously, but some not, which may be caused by the interaction between the charge density changes of different Fe ions.

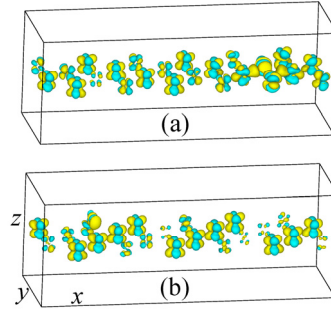


Fig. 5 CDD of the 6×2 supercell from Li^+ Insertion (GGA+U, iso = 0.01) (a) and Slight Change (GGA+U, iso = 0.01) (b)

3.3 $\text{Nd}_2\text{Fe}_2\text{As}_2\text{O}_2$

For the investigation of $\text{Nd}_2\text{Fe}_2\text{As}_2\text{O}_2$, the k -point is set to $10 \times 10 \times 5$. Since Nd is a $4f$ transition metal atom, it has strong spin-orbital coupling and strong correlation. The spin-orbital coupling effect is considered in the calculation and the strong correlation effect is described by the GGA+U method ($U_{\text{eff}} = 7.0$ eV). The calculation of uniform electric field together with spin-orbital coupling may be too expensive, so the author gives only the result of inserting one Li^+ ion.

The Li^+ ion is located at (0.5, 0.25, 0.317), which is 1.912 Å, 1.927 Å, and 2.281 Å from the nearest Nd, Fe, and As, respectively. The author also gives the results when the Li^+ ion is closer to one Nd atom. The coordinate of the Li^+ ion is (0.4, 0.4, 0.2) and it is 1.54 Å from the nearest Nd atom. Fig. 6 shows the CDDs. When the distance between the Li^+ ion and the Nd atom is large, rotation of the electron cloud of the Nd ion cannot be observed. When the distance decreased, obvious change appears. This suggests that the $4f$ electron cloud of Nd may also play an important role in superconductivity.

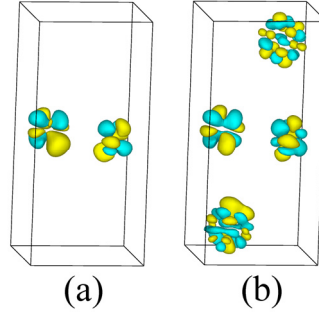


Fig. 6 CDDs from Li^+ Insertion (GGA+U, iso = 0.02). Li^+ ion is 1.912 Å (a) and 1.54 Å (b) from the nearest Nd atom, respectively.

3.4 $\text{Ba}_{1-x}\text{K}_x\text{Fe}_2\text{As}_2$

The T_c of $\text{Ba}_{1-x}\text{K}_x\text{Fe}_2\text{As}_2$ can reach 38K^[42]. $\text{Ba}_2\text{Fe}_4\text{As}_4$ and $\text{BaKFe}_4\text{As}_4$ were employed in the calculation, corresponding to $x = 0$ and 0.5, respectively. For the valence state of $\text{Ba}_2\text{Fe}_4\text{As}_4$, As is -3, Ba is +2, and Fe is +2. For $\text{BaKFe}_4\text{As}_4$, As is -3, Ba is +2, K is +1 and Fe is +9/4. The k -point is set to $10 \times 10 \times 4$ when using the GGA+U method and $6 \times 6 \times 2$ when using the HSE method. Fig. 7 shows the DOS of $\text{Ba}_2\text{Fe}_4\text{As}_4$. The two methods are in good agreement, except that the GGA+U method gives a lower bandgap.

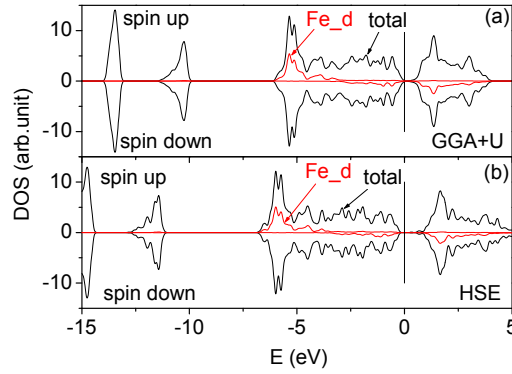


Fig. 7 DOS of $\text{Ba}_2\text{Fe}_4\text{As}_4$ from GGA+U (a) and HSE (b) method

Two methods were used to calculate the electric field effect. One is to insert one Li^+ ion. The coordinate is (0.5,0.5,0.69), and it is 2.470 Å, 2.191 Å, and 2.268 Å away from the nearest neighbor Ba, As, and Fe, respectively. The other is to apply a uniform electric field by the QE package, in which k -point is set to $6 \times 6 \times 2$. The value and direction of the electric field are the same as those given above. The convergence reaches 1×10^{-4} Ha. Fig. 8 shows the crystal structure and the results, in which the CDD of $\text{BaKAs}_4\text{Fe}_4$ from Li^+ Insertion is also given. The rotation of the charge densities of Fe ions is obvious.

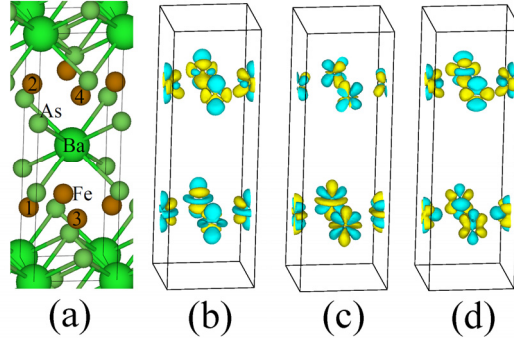


Fig. 8 (a) Crystal structure of $\text{Ba}_2\text{Fe}_4\text{As}_4$; (b) CDD of $\text{Ba}_2\text{Fe}_4\text{As}_4$ from Li^+ Insertion (GGA+U, iso = 0.02); (c) CDD of $\text{Ba}_2\text{Fe}_4\text{As}_4$ from Uniform E-field (QE, GGA+U, iso = 0.02); (d) CDD of $\text{BaKAs}_4\text{Fe}_4$ from Li^+ Insertion (GGA+U, iso = 0.02)

For $\text{BaKAs}_4\text{Fe}_4$, apparent charge density rotation can also be observed when the position of an As atom is slightly changed or a uniform electric field is applied

3.5 ($\text{YBa}_2\text{Cu}_3\text{O}_7$)₂

To access an antiferromagnetic state, $(\text{YBa}_2\text{Cu}_3\text{O}_7)_2$ was used, no electron added or subtracted. When the GGA+U method is adopted, the k -point is set to $8 \times 8 \times 4$. When the HSE method is used, the k -point is $4 \times 4 \times 2$. Fig. 9 shows the DOS.

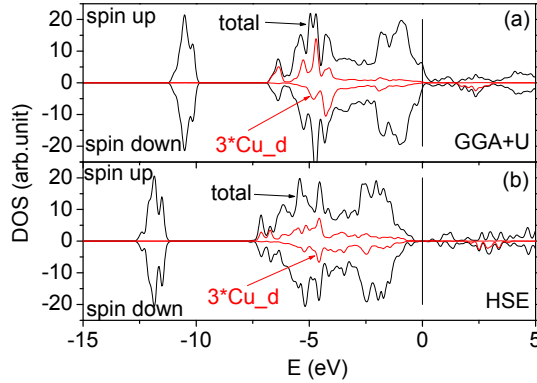


Fig. 9 DOS of $(\text{YBa}_2\text{Cu}_3\text{O}_7)_2$ from GGA+U (a) and HSE (b) method. Cu_d has been multiplied by 3 for clarity.

The spin density of the system was calculated. The effect of an electric field induced by a slight change in the position of one oxygen atom in the copper oxide plane was calculated. The original coordinate of the oxygen atom was (0.75, 0.25, 0.62245), and then changed to (0.8, 0.3, 0.62245). The position was changed in the (110) direction by 0.39 Å. The method is GGA+U, and the result was validated by HSE. The author also performed the calculation for the vertical change (0.23 Å) of the oxygen atom. Substituting Cu with Zn was also calculated with the GGA+U method (3d electrons of Zn are regarded as valence electrons and set $U_{\text{eff}} = 6.5\text{eV}$), and the position of oxygen atom was changed along (110). Fig. 10 shows the crystal structure and results.

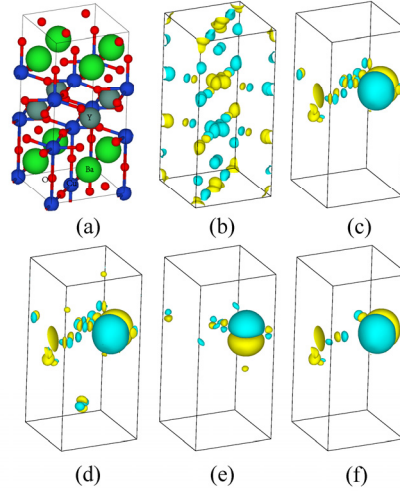


Fig. 10 (a) Crystal structure; (b) Spin density map (GGA+U, iso = 0.01); (c) CDD form Slight Change (GGA+U, iso = 0.004); (d) CDD from Slight Change (HSE, iso = 0.004); (e) CDD from Slight Change along z direction (GGA+U, iso = 0.004); (f) CDD of YBaZnO from Slight Change (GGA+U, $U_{\text{eff}} = 6.5\text{eV}$, iso = 0.004)

It can be seen from the spin density map that the Cu ions in the copper-oxygen layer exhibit an antiferromagnetic state. The electron cloud of Cu ions shows an obvious rotation. It is worth noting that the isosurface is about one order of magnitude smaller than that of Fe ions in iron-based superconductors. The electron cloud of Zn did not rotate at all. Calculations with $U_{\text{eff}} = 0$ show that the electron cloud of Zn does not rotate too. Table 3 gives the LMM of the Cu atom. When the electric field is not applied, the results given by the GGA+U and the HSE method are very consistent. When there is an influence, the change of the LMM is very small.

Table 3 LMM of the Cu atom in $(\text{YBa}_2\text{Cu}_3\text{O}_7)_2$

| | Method | Cu |
|--------------|------------------|-------|
| GGA+U | No field | 0.634 |
| | Slight Change xy | 0.631 |
| | Slight Change z | 0.641 |
| HSE | No field | 0.631 |

The rotation is also observed in $(\text{YBa}_2\text{Cu}_3\text{O}_7)_2$ with 0.3 or 2 electrons added. The author believes that, if the 3d orbitals of Cu is not fully filled, the electron will rotate under electric fields. When the 3d shell is filled, the rotation cannot be observed.

3.6 $(\text{HgBa}_2\text{Ca}_2\text{Cu}_3\text{O}_8)_2$

To achieve an antiferromagnetic state, $(\text{HgBa}_2\text{Ca}_2\text{Cu}_3\text{O}_8)_2$ was used. No electrons were added or subtracted. With the GGA+U method, the k -point is set to $8 \times 8 \times 4$. With the HSE method, the k -point is set to $4 \times 4 \times 2$. Fig. 11 shows the DOS. The 3d orbital of Cu (Cu_d) is of the middle copper-oxide layer.

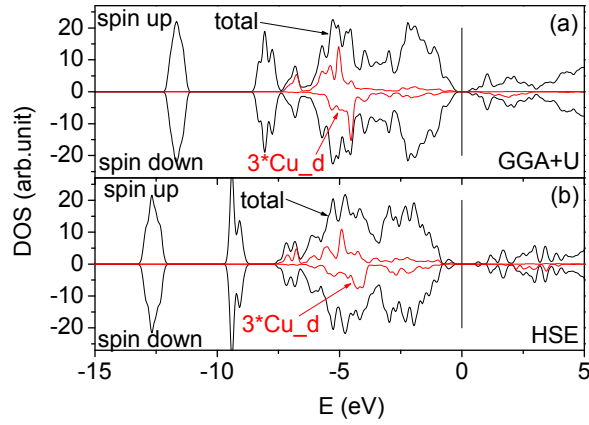


Fig. 11 DOS of $(\text{HgBa}_2\text{Ca}_2\text{Cu}_3\text{O}_8)_2$ from GGA+U (a) and HSE (b) method.

The effect of electric fields is calculated by slightly changing one oxygen atom in the middle copper-oxygen layer. The original position of the oxygen atom is (0.75, 0.25, 0.5) and then changed to (0.8, 0.3, 0.5). The position was changed in the (110) direction by 0.39 Å. The result was verified by the HSE method. Fig. 12 shows the crystal structure, spin density map and CDDs with and without electric fields. The charge density of Cu ions exhibits clear rotations and the GGA+U method gives consistent result with the HSE method.

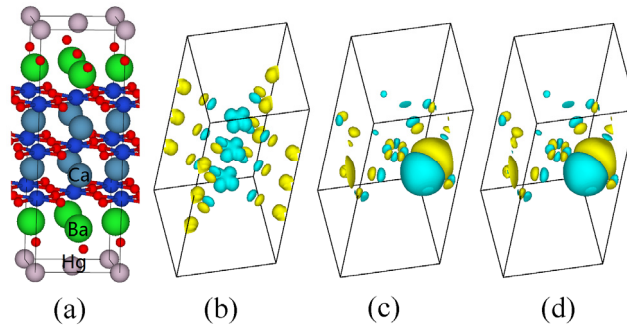


Fig. 12 (a) Crystal structure; (b) Spin density map (HSE, iso = 0.01); (c) CDD from Slight Change (GGA+U, iso = 0.003); (d) CDD from Slight Change (HSE, iso = 0.003)

Table 4 gives the LMM. Consistency between the HSE and GGA+U method can be seen and the effect of a Slight Change on the LMM is very small.

Table 4 LMM of the Cu atom in $(\text{HgBa}_2\text{Ca}_2\text{Cu}_3\text{O}_8)_2$

| | Method | Cu |
|--------------|---------------|-------|
| GGA+U | No field | 0.603 |
| | Slight Change | 0.600 |
| HSE | No field | 0.618 |
| | Slight Change | 0.619 |

Calculations of $(\text{HgBa}_2\text{Ca}_2\text{Cu}_3\text{O}_9)_2/(\text{HgBa}_2\text{Ca}_2\text{Cu}_3\text{O}_9+2\text{e})_2$ show that there are significant rotations of the electron cloud of copper atoms.

Further, a $4\times 1\times 1$ supercell of $(\text{HgBa}_2\text{Ca}_2\text{Cu}_3\text{O}_8)_2$ was calculated. The original coordinate of the oxygen atom to be changed is (0.1875, 0.25, 0.5), and then changed to (0.2, 0.3, 0.5). The CDD is displayed in Fig. 13. There is a clear rotation on Cu atom. However, no rotation occurs far away from where the influence is applied. This is totally different from that of iron-based superconductors. For iron-based superconductors, rotation can be observed further away.



Fig. 13 CDD of the $4\times 1\times 1$ supercell from Slight Change (GGA+U, iso = 0.003)

3.7 $(\text{Tl}_2\text{Ba}_2\text{CaCu}_2\text{O}_8)_4$

To access an antiferromagnetic state, the author adopted $(\text{Tl}_2\text{Ba}_2\text{CaCu}_2\text{O}_8)_4$, no electron added or subtracted. The GGA+U method is used, and the k -point is set to $6\times 6\times 1$. Fig. 14 shows the DOS.

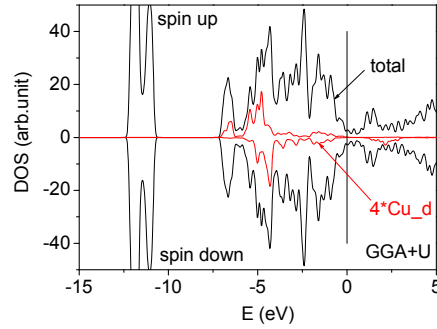


Fig. 14 DOS of $(\text{Tl}_2\text{Ba}_2\text{CaCu}_2\text{O}_8)_4$ from GGA+U method

The position of the O atom was changed by 0.39 Å, -0.39 Å and 0.78 Å, respectively, in the (110) direction. Fig. 15 displays the CDDs. It can be clearly seen that the electron cloud of the Cu^{2+} ion rotates with the change of the O atom's position. Slightly changing the position of oxygen atoms near Tl or Ba, the author did not observe the rotation of the electron cloud of Tl or Ba.

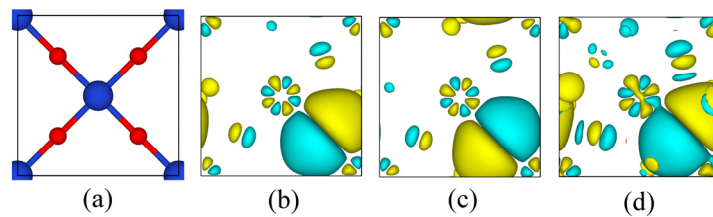


Fig. 15 (a) Copper-oxygen layer; (b) CDD from Slight Change of 0.39 Å; (c) CDD from Slight Change of -0.39 Å;

(c) CDD from Slight Change of 0.78Å (GGA+U, iso = 0.003)

3.8 (Bi₂Sr₂Ca₂Cu₃O₁₀)₄

(Bi₂Sr₂Ca₂Cu₃O₁₀)₄ was adopted, no electron added or subtracted. The k -point is set to 5×5×1.

Fig. 16 shows the DOS.

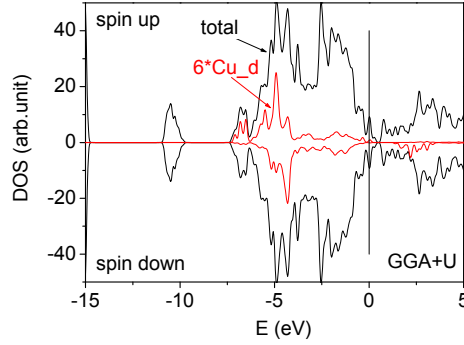


Fig. 16 DOS of (Bi₂Sr₂Ca₂Cu₃O₁₀)₄ from GGA+U method

The system has three adjacent copper-oxygen layers, the position of one oxygen atom in the uppermost copper-oxygen layer is changed. The original coordinate is (0.75, 0.25, 0.586189), and then changed to (0.8, 0.3, 0.586189). The author also studied the case of increasing or decreasing the lattice constant. Fig. 17 shows the results. There is also a significant rotation of the electron cloud of Cu ions when the lattice constant is increased or decreased.

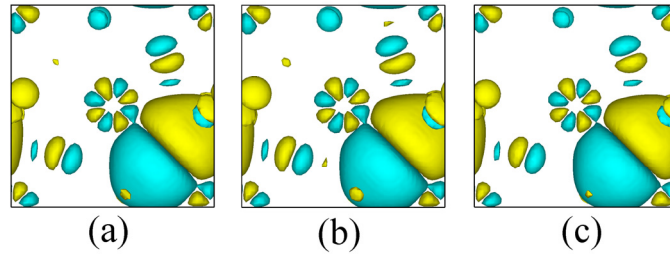


Fig. 17 (a) CDD from Slight Change (GGA+U, iso = 0.002), (b) The lattice constant decreases by 2.5%; (c) The lattice constant increases by 2.5%

It can be seen from the results of the above eight systems all the electron clouds of Cu ions or Fe ions have obvious changes under electric fields. The author believes this change should be called a rotation not an elastic deformation, because the CDD does not simply follow the direction of the electric field, but increases in some areas and decreases in others.

Is this rotation just of 3d (or 4f) electron cloud? Considering the orthogonality of the atomic orbitals, the author thinks a change of the outer electron clouds will inevitably affect the inner electron clouds. So, the inner electron cloud will rotate too. However, the rotation of the inner electron cloud is difficult to observe because they have spherical symmetry.

Why do electron clouds rotate? We know that transition metal ions (3d or 4f) have incompletely filled 3d or 4f orbitals. The electron cloud does not have perfect spherical symmetry.

It is like a polar molecule and will rotate under electric fields.

In addition to the above eight typical unconventional superconductors, other superconductors, such as metallic Nb, heavy fermion superconductor UPt_3 , rare earth superconductor SmRh_4B_4 , et al., have incompletely filled $3d$ or $4f$ shells. They are likely to rotate under an electric field and thus play an important role in superconducting electron pairing.

4. Possible Superconducting Electron Pairing Mechanism, Views on some issues, and Research Prospect

4.1 Mechanism

Mr. Anderson has raised the issue of whether a glue exists in high temperature superconductors. The author believes it does exist. Combined with the simple and intuitive model of electron-phonon interaction and the fact that transition-metal ions' electron clouds rotate under an electric field, the author proposes that the rotation of the transition metal electron cloud is the glue. When an electron comes to a new location, the electron cloud of the transition metal ions in the vicinity will rotate. In this way, the charge density around the electron will decrease (equivalent to the emergence of a positive charge). When the electron leaves, the electron cloud of the transition metal ions *will not relax immediately (it is so crucial that that the author will discuss it later)*, so that there will be a region lack of charge (equivalent to a positive charge region) that will attract another electron. Attraction between electrons appears. This mechanism is essentially the same as the electron-phonon interaction, except that the medium is the rotation of the electron cloud, not the displacement of ions.

4.2 Author's views on some issues

4.2.1 Relaxation time of the electron cloud rotation

The most important point in the new pairing mechanism is the relaxation time of the electron cloud's rotation. If the relaxation time is smaller than that of the elastic deformation of the electron cloud, then it cannot be the glue. The author believes that this relaxation time will not be so small, because the inner electrons will also rotate due to the requirement of orthogonality of electron wavefunctions. This is the most important follow-up study.

4.2.2 Is the rotation of electron clouds of ions or ions?

The author think 'Rotation of ions' is better, because it is more simple and intuitive.

4.2.3 The role of strong correlation

For the electron cloud rotation, iron-based superconductors are more obvious than copper-based superconductors, but the T_c of copper-based superconductors is higher than that of iron-based superconductors. In addition to different electronic structures, the author believes that the strong correlation plays an important role. Copper-based superconductors have stronger

correlation effect than iron-based superconductors. The screening is strong in iron-based superconductors, which causes a lower T_c . For the relationship between strong correlation and high T_c , the author believes strong correlation is a necessary but not sufficient condition for high T_c . In strongly correlated systems, electrons cannot be described by free electrons or weakly interacting quasi-particles, so that a strong attraction is possible. The screening in traditional superconductors is strong, on the one hand reducing the repulsion between electrons, but also lead to a weak attraction.

4.2.4 Relationship between magnetism and unconventional superconductivity

The author thinks that the rotation of the electron cloud of transition metal ions is the fundamental reason for the unconventional superconductivity. The rotation is because the atomic shells are not fully filled and no spherical symmetry present. When there is an electric field, it will rotate. Magnetism is also because the shells are not fully filled.

4.3 Research prospect

4.3.1 The research in this article is mainly concentrated on the existence of the electron cloud rotation. More detailed researches are needed. For example, the projected DOS and more analysis should be given. In addition, the study also need more accurate calculations, such as the use of the Quantum Monte Carlo method. Most results of this paper are qualitative. Further research requires quantitative analysis, such as quantification of the applied electric field and quantification of the electron cloud rotation.

4.3.2 The author believes that determination of the relaxation time of the electron cloud rotation is crucial. Theoretical and experimental studies of the electron cloud rotation and the relaxation time should be given.

4.4.3 New theories and application. For example, theory of the interaction between electrons and the rotation of ions, possible long-range modes of the rotation in iron-based superconductors, and influence (or application) of rotation of transition metal ions in other fields.

4. Conclusion

The author studied eight typical unconventional superconductors. The electron cloud of transition metal ions is found to rotate under electric fields. Extensive calculations show that if there is an incompletely filled electronic orbital, the electron cloud will rotate. If the orbital is filled, the electron cloud will not rotate. The authors believe that the rotation of transition metal ion's electron cloud may be a new medium of superconducting electron pairing, just as lattice deformation is the conventional superconducting electron pairing medium. The author's views on this new possible pairing mechanism, strong correlation and superconductivity, magnetism and superconductivity, and follow up studies are given.

References

- [1] Bednorz, J. G., Müller, K. A.: Possible high T_C superconductivity in the Ba-La-Cu-O system. *Zeitschrift für Physik B* 64, 189-193 (1986)
- [2] Wu, M. K., Ashburn, J. R., Torng, C. J., Hor, P. H., Meng, R. L., Gao, L., Huang, Z. J., Wang, Y. Q., Chu, C. W.: Superconductivity at 93 K in a new mixed-phase Y-Ba-Cu-O compound system at ambient pressure. *Physical Review Letters* 58, 908-910 (1987)
- [3] Zhao, Z. X., Chen, L. Q., Yang, Q. S., Huang, Y. Z., Chen, G. H., Tang, R. M., Liu, G. R., Cui, C. G., Chen, L., Wang, L. Z., Guo, S. Q., Li, S. L., Bi, J. Q.: Superconductivity above liquid-nitrogen temperature in Ba-Y-Cu oxides. *Chinese Science Bulletin* 6, 412-414 (1987)
- [4] Maeda, H., Tanaka, Y., Fukutumi, M., Asano, T.: A New High- T_c Oxide Superconductor without a Rare Earth Element. *Japanese Journal of Applied Physics* 27, L209-L210 (1988)
- [5] Sheng, Z. Z., Hermann, A. M.: Bulk superconductivity at 120 K in the Tl-Ca/Ba-Cu-O system. *Nature* 332, 138-139 (1988)
- [6] Sheng, Z. Z., Hermann, A. M., El Ali, A., Almasan, C., Estrada, J., Datta, T., Matson, R. J.: Superconductivity at 90 K in the Tl-Ba-Cu-O system. *Physical Review Letters* 60, 937-940 (1988)
- [7] Putilin, S. N., Antipov, E. V., Chmaissem, O., Marezio, M.: Superconductivity at 94 K in $\text{HgBa}_2\text{CuO}_{4+\delta}$. *Nature* 362, 226-228 (1993)
- [8] Schilling, A., Cantoni, M., Guo, J. D., Ott, H. R.: Superconductivity above 130 K in the Hg-Ba-Ca-Cu-O system. *Nature* 363, 56-58 (1993)
- [9] Chu, C. W., Gao, L., Chen, F., Huang, Z. J., Meng, R. L., Xue, Y. Y.: Superconductivity above 150 K in $\text{HgBa}_2\text{Ca}_2\text{Cu}_3\text{O}_{8+\delta}$ at high pressures. *Nature* 365, 323-325 (1993)
- [10] Kamihara, Y., Hiramatsu, H., Hirano, M., Kawamura, R., Yanagi, H., Kamiya, T., Hosono, H.: Iron-Based Layered Superconductor: LaOFeP . *Journal of the American Chemical Society* 128, 10012-10013 (2006)
- [11] Kamihara, Y., Watanabe, T., Hirano, M., Hosono, H.: Iron-Based Layered Superconductor $\text{La}[\text{O}_{1-x}\text{F}_x]\text{FeAs}$ ($x = 0.05-0.12$) with $T_c = 26$ K. *Journal of the American Chemical Society* 130, 3296-3297 (2008).
- [12] Ozawa, T. C., Kauzlarich, S. M.: Chemistry of layered d -metal pnictide oxides and their potential as candidates for new superconductors. *Science and Technology of Advanced Materials* 9, 033003 (2008)
- [13] Ren, Z. A., Yang, J., Lu, W., Yi, W., Che, G. C., Dong, X. L., Sun, L. L., Zhao, Z. X.: Superconductivity at 52 K in iron based F doped layered quaternary compound $\text{Pr}[\text{O}_{1-x}\text{F}_x]\text{FeAs}$. *Materials Research Innovations* 12, 105-106 (2008)

- [14] Ren, Z. A., Che, G. C., Dong, X. L., Yang, J., Lu, W., Yi, W., Shen, X. L., Li, Z. C., Sun, L. L., Zhou, F., Zhao, Z. X.: Superconductivity and phase diagram in iron-based arsenic-oxides $\text{ReFeAsO}_{1-\delta}$ (Re = rare-earth metal) without fluorine doping. *Europhysics Letters* 83, 17002 (2008)
- [15] Wang, Q. Y., Li, Z., Zhang, W. H., Zhang, Z. C., Zhang, J. S., Li, W., Ding, H., Ou, Y. B., Deng, P., Chang, K., Wen, J., Song, C. L., He, K., Jia, J. F., Ji, S. H., Wang, Y. Y., Wang, L. L., Chen, X., Ma, X. C., Xue, Q. K.: Interface-Induced High-Temperature Superconductivity in Single Unit-Cell FeSe Films on SrTiO_3 . *Chinese Physics Letters* 29, 037402 (2012)
- [16] Ge, J. F., Liu, Z. L., Liu, C. H., Gao, C. L., Qian, D., Xue, Q. K., Liu, Y., Jia, J. F.: Superconductivity above 100 K in single-layer FeSe films on doped SrTiO_3 . *Nature Materials* 14, 285–289 (2015)
- [17] Anderson, P. W.: The resonating valence bond state in La_2CuO_4 and superconductivity. *Science* 235, 1196–1198 (1987)
- [18] Anderson, P. W.: Twenty years of talking past each other: the theory of high T_c . *Physica C* 460, 3–6 (2007)
- [19] Monthoux, P., Balatsky, A., Pines, D.: Weak-coupling theory of high-temperature superconductivity in the antiferromagnetically correlated copper oxides. *Physical Review B* 46, 14803–14817 (1992)
- [20] Chakravarty, S., Sudbø, A., Anderson, P. W., Strong, S.: Interlayer Tunneling and Gap Anisotropy in High-Temperature Superconductors. *Science* 261, 337–340 (1993).
- [21] Anderson, P. W.: Is There Glue in Cuprate Superconductors? *Science* 22, 1705-1707 (2007)
- [22] Fröhlich, H.. Theory of the Superconducting State. I. The Ground State at the Absolute Zero of Temperature. *Physical Review* 79, 845-856(1950)
- [23] Reynolds, C. A., Serin, B., Wright, W. H., Nesbitt, L. B.: Superconductivity of Isotopes of Mercury. *Physical Review* 78, 487 (1950)
- [24] Maxwell, E.: Isotope Effect in the Superconductivity of Mercury. *Physical Review* 78, 477 (1950)
- [25] Bardeen, J., Cooper, L. N., Schrieffer, J. R.: Microscopic Theory of Superconductivity. *Physical Review* 106, 162–164 (1957)
- [26] Bardeen, J., Cooper, L. N., Schrieffer, J. R.: Theory of Superconductivity. *Physical Review* 108, 1175–1204 (1957)
- [27] Xi, X. X., Li, Q., Doughty, C., Kwon, C., Bhattacharya, S., Findikoglu, A. T., Venkatesan, T.: Electric field effect in high T_c superconducting ultrathin $\text{YBa}_2\text{Cu}_3\text{O}_{7-x}$ films. *Applied Physics Letters* 59, 3470-3472 (1991)

- [28] Mannhart, J., Bednorz, J. G., Müller, K. A., Schlom, D. G., Ströbel, J.: Electric field effect in high- T_c superconductors. *Journal of Alloys and Compounds* 195, 519-525 (1993)
- [29] Orlova T. S., Kudymov, A. N., Smirnov, B. I., Miller, D. J., Lanagan, M. T., Goretta, K. C.: Electric field effects on the conductivity of highly textured $\text{Bi}_2\text{Sr}_2\text{CaCu}_2\text{O}_y$. *Physica C* 253, 194-198 (1995)
- [30] Kresse, G., Hafner, J.: Ab initio molecular dynamics for liquid metals. *Physical Review B* 47, 558–561 (1993)
- [31] Kresse, G., Furthmüller, J.: Efficient iterative schemes for ab initio total-energy calculations using a plane-wave basis set. *Physical Review B* 54, 11169–11186 (1996)
- [32] Blöchl, P.E.: Projector augmented-wave method. *Physical Review B* 50, 17953–17979 (1994)
- [33] Kresse, G., Joubert, D.: From ultrasoft pseudopotentials to the projector augmented-wave method. *Physical Review B* 59, 1758–1775 (1999)
- [34] Perdew, J. P., Burke, K., Ernzerhof, M.: Generalized Gradient Approximation Made Simple. *Physical Review Letters* 77, 3865 (1996)
- [35] Anisimov, V. I., Korotin, Dm. M., Streltsov, S. V., Kozhevnikov, A. V., Kuneš, J., Shorikov, A. O., Korotin, M. A.: Density-functional calculation of the Coulomb repulsion and correlation strength in superconducting LaFeAsO . *JETP Letters* 88, 729–733 (2008)
- [36] Qian, M. C., Hu, W. Y., Zheng, Q. Q.: Electronic structure of $\text{PrBa}_2\text{Cu}_3\text{O}_7$ and $\text{YBa}_2\text{Cu}_3\text{O}_7$: A local spin density approximation with the on-site Coulomb interaction study. *Journal of Applied Physics* 85, 4765-4767 (1999)
- [37] Blaha P., Schwarz, K., Novák, P.: Electric Field Gradients in Cuprates: Does LDA+U Give the Correct Charge Distribution? *International Journal of Quantum Chemistry* 101, 550–556 (2005)
- [38] Heyd, J., Scuseria, G. E., Ernzerhof, M.: Hybrid functionals based on a screened Coulomb potential. *Journal of Chemical Physics* 118, 8207–8215(2003)
- [39] Giannozzi, P., Baroni, S., Bonini, N., Calandra, M., Car, R., Cavazzoni, C., Ceresoli, D., Chiarotti, G. L., Cococcioni, M., Dabo, I., Corso, A. D., de Gironcoli, S., Fabris, S., Fratesi, G., Gebauer, R., Gerstmann, U., Gougoussis, C., Kokalj, A., Lazzeri, M., Martin-Samos, L., Marzari, N., Mauri, F., Mazzarello, R., Paolini, S., Pasquarello, A., Paulatto, L., Sbraccia, C., Scandolo, S., Sclauzero, G., Seitsonen, A. P., Smogunov, A., Umari, P., Wentzcovitch, R. M.: QUANTUM ESPRESSO: a modular and open-source software project for quantum simulations of materials. *Journal of Physics: Condensed Matter* 21, 395502 (2009)
- [40] Ricci, A., Poccia, N., Joseph, B., Arrighetti, G., Barba, L., Plaisier, J., Campi, G., Mizuguchi, Y., Takeya, H., Takano, Y., Saini, Lal N., Bianconi, A.: Intrinsic phase separation in superconducting $\text{K}_{0.8}\text{Fe}_{1.6}\text{Se}_2$ ($T_c = 31.8$ K) single crystals. *Superconductor Science and Technology* 24, 082002 (2011)

[41] Guo, J. G., Jin, S. F., Wang, G., Wang, S. C., Zhu, K. X., Zhou, T. T., He, M., Chen, X. L.: Superconductivity in the iron selenide $K_xFe_2Se_2$ ($0 \leq x \leq 1.0$). Physical Review B 82, 180520(R) (2010).

[42] Rotter, M., Tegel, M., Johrendt, D.: Superconductivity at 38 K in the Iron Arsenide $(Ba_{1-x}K_x)Fe_2As_2$. Physical Review Letters 101, 107006 (2008)